Journal of Alloys and Compounds 577S (2013) S517–S520

Contents lists available at ScienceDirect

Journal of Alloys and Compounds

journal homepage: www.elsevier.com/locate/jallcom

Effect of thermal and mechanical cycling on the elastic and dissipative energy in CuAl(11.5wt%)Ni(5.0wt%) shape memory alloy

T.Y. Elrasasi*, M.M. Dobróka, L. Daróczi, D.L. Beke

Department of Solid State Physics, University of Debrecen, P.O. Box 2, H-4010 Debrecen, Hungary

ARTICLE INFO

Article history:
Available online 30 June 2012

Keywords:
Shape memory
Martensitic transformation
Effect of cycling

ABSTRACT

Effect of thermal and mechanical cycling on β/β′ phase transformation in CuAl(11.5 wt%)Ni(5.0 wt%) single crystalline shape memory alloy was studied. The ε–σ and ξ–T hysteretic loops were investigated after different numbers of thermal and mechanical cycles (ε and ξ are the relative deformation and martensite fraction respectively, σ and T denote the stress and temperature). The ε–σ loops were determined at fixed temperature (373 K). The ξ–T loops under zero stress were calculated from the DSC curves measured. The elastic and the dissipative energy contributions, following the procedure given in [1,2], were calculated as the function of the transformed fraction for both types of the hysteretic loops. Finally the dependence of the total elastic, E, and dissipative energy, D, (per one cycle) on the cycling number was calculated. In thermal cycling E increased by about 12 J/mol, and D decreased by about 6 J/mol. On the other hand for mechanical cycling E decreased by about 6 J/mol and D increased by about 0.2 J/mol.

1. Introduction

Shape memory alloys (SMA) have important technological applications as functional smart materials (see e.g. [3–6]). Especially two alloy families have been commonly used for mass industrial applications, the Ti–Ni and Cu-base alloys [3–5,7,8]. These applications imply a deep knowledge of the characteristics of the thermoelastic martensitic transformation, which provides the basis mechanism for shape memory behavior. Thus deeper understanding of the cycling and stress effects on the transformation can lead to improved control of the shape memory function. Many applications of shape memory devices require a large number of thermal and mechanical cycles and also a stable and reliable shape memory effect. As a first step to understanding of the basic mechanisms of fatigue we carried out investigations on the effect of number of thermal and stress driven cycling on the β/β' phase transformation in single crystalline CuAl(11.5 wt%)Ni(5.0 wt%) alloy.

2. Experimental

Characteristics of the thermoelastic martensitic transformation have been studied in CuAl(11.5 wt%)Ni(5.0 wt%) single crystalline shape memory alloys. Effect of cycling on stress induced martensitic transformations was investigated under uniaxial stress at constant temperature (373 K). The sample was cut from a rod by a simple electro discharge machine and the final dimensions were: 50 mm in length and 0.59 mm^2 in square cross section. The [110] direction was parallel to the axis of the rod and the direction of the applied stress. The stress–strain curves were obtained by a tensile machine (Chatillon TCD225) applying an external heating system in which thermal resistance was used for heating. The transformed martensite fraction versus temperature curves as well as the heat of transformations, Q, at zero stress were obtained from the measured differential scanning calorimeter, DSC, runs (Perkin-Elmer DSC-7) at zero uniaxial stress with 10 K/min heating and cooling rate. The method described in [6] was used to obtain ξ as the function of temperature both for cooling and heating, by taking the ratio of the partial and full integral of the DSC curves (integrating Q/T between, e.g. the martensite start temperature, M_s, and T as well as between M_s and martensite finish, M_f temperature, respectively). Fig. 1 shows the DCS curve and the $\xi(T)$ hysteretic curve calculated. The entropy of the phase transformation was calculated also from the integrals of the cooling down and heating up Q/T curves:

$$\Delta S^{A/M} = \int_{M_s}^{M_f} (dQ^{M/A}/T) \approx -\Delta S^{M/A} = \int_{A_s}^{A_f} (dQ^{M/A}/T)$$

and $\Delta S = \Delta S^{A/M} = -1.26$ J/mol K was obtained and its magnitude was the same for heating and cooling. Superscript A/M indicates that ΔS belongs to the austenite to martensite transition and a similar relation holds for the reverse process with M/A. Furthermore the values of ΔS were equal to each other within the experiential errors after different numbers of cycling, N, i.e. ΔS was independent of N.

3. Results

3.1. Dsc measurements

Fig. 2 shows the normalized ξ–T hysteretic loops calculated from the DSC curves for three different N. It can be seen that both the area of the loops and the slopes of the upper and lower branches have systematic changes with N.

---

* Corresponding author.
E-mail address: tarekyousif75@gmail.com (T.Y. Elrasasi).

0925-8388/$ – see front matter © 2012 Elsevier B.V. All rights reserved.
http://dx.doi.org/10.1016/j.jallcom.2012.06.108

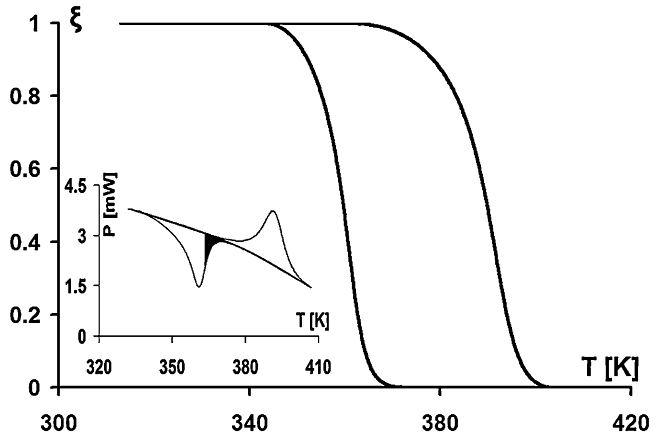

Fig. 1. Hysteresis, ξ (T), loop calculated from the DSC curves (shown in the insert).

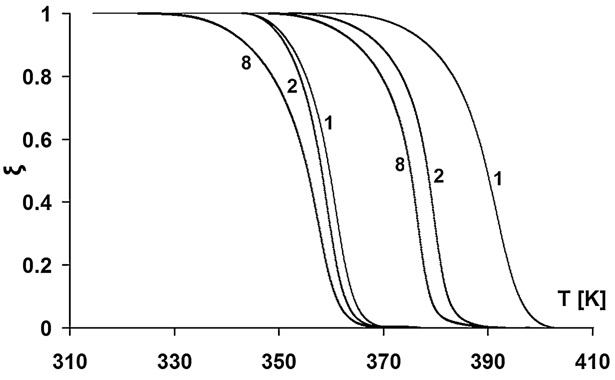

Fig. 2. Hysteresis loops calculated from the DSC curves.

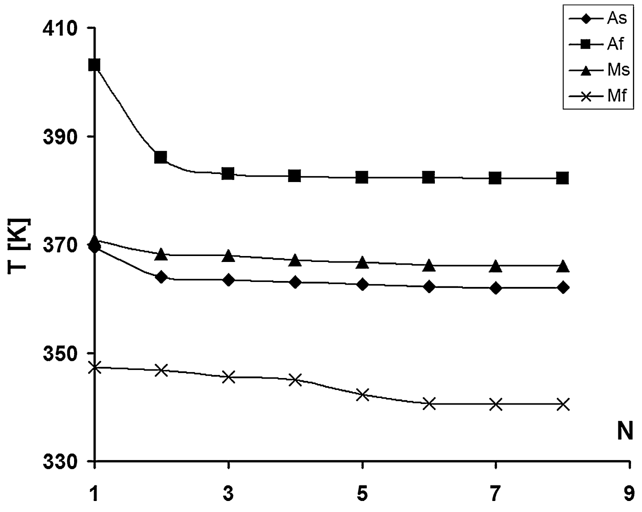

Fig. 3. Start and finish temperatures as the function cycle number.

Fig. 3 shows the start and finish temperatures as the function of the number of cycles, N. It can be seen that there is a considerable shift in A_f and A_s temperatures after the first one/two cycles.

On the basis of a local equilibrium formalism and thermoelastic balance [7,9], relations for the elastic and dissipative energy contributions to the up (A/M) and down (M/A) branches of the hysteresis loops were derived in [1,2]. It was obtained that the inverses of the ξ–T loops can be given as

$$T^{A/M}(\xi) = T_0(\sigma) - [d(\xi) + e(\xi)]/[-\Delta s]$$

$$T^{M/A}(\xi) = T_0(\sigma) - [d(\xi) + e(\xi)]/[-\Delta s] \qquad (1)$$

where $d(\xi) = \partial D/\partial\xi$, as well as $e(\xi) = \partial E/\partial\xi$, with D and E being the total dissipative and elastic energies per cycle, respectively. In deriving relations (1) $e(\xi) = e(\xi)^{A/M} = -e(\xi)^{M/A}$ and $d(\xi) = d(\xi)^{A/M} = d(\xi)^{M/A}$ assumptions, usually applied in shape memory alloys, were made [1,2]. Furthermore, the stress dependence of the equilibrium transformation temperature, T_o, is given by the Clausius–Clapeyron relation

$$T_o(\sigma) = T_o(0) + V\varepsilon^{tr}(\sigma)/(-\Delta s), \qquad (2)$$

where $\varepsilon^{tr} = \varepsilon^{tr}{}_{A/M} = -\varepsilon^{tr}{}_{M/A}$ is the transformation strain and V is the molar volume. In general the transformation strain, ε^{tr}, – in contrast e.g. to the entropy of phase transformation – depends on the stress [2] and thus ε^{tr} should be taken at that fixed σ at which the ξ–T loop is measured. The stress and temperature dependence of ε^{tr} for this alloy was determined in our previous paper (see Figs. 2b and 3b in [10]) and these results will be used here too. The start and finish temperatures can be obtained from Eq. (1) taking it at $\xi = 0$ and 1, respectively.

According to Eq. (1) the ξ dependence of the elastic and dissipative energy can be obtained from the sum and difference of $T^{M/A}$ and $T^{A/M}$ curves, respectively. Fig. 4a and b show the total elastic, E, and dissipative, D, energies, as calculated from the integrals of the above curves (between $\xi = 0$ and 1), versus N. Note that E can be calculated only irrespective of the $T_o\Delta S$, thus on Fig. 4a $E + T_o\Delta S$ is plotted. On other hand, by using the well-known relations $Q^{A/M} + Q^{M/A} = 2D$ and $Q^{A/M} - Q^{M/A} = 2E + 2T_o\Delta S$, one can also get the same results, which are also shown on Fig. 4a and b. It can be seen, as expected, that these points fit well to the $Q^{M/A} - Q_{A/M}$ and $Q^{M/A} + Q^{A/M}$ values (calculated from the integrals of the DSC curves), respectively.

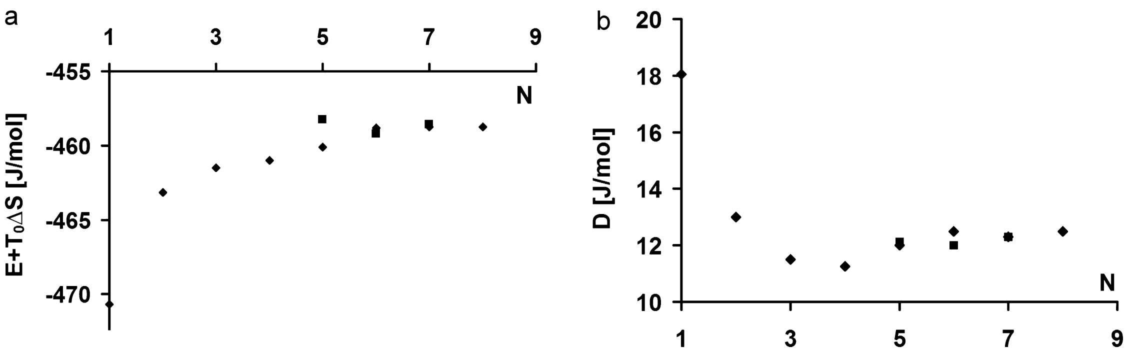

Fig. 4. Cycle number dependence of the total elastic energy (a) and the total dissipative energy (b) for thermal cycles [♦ obtained from the ξ–T loops, ■ obtained from the heats of transformation; see also the text].

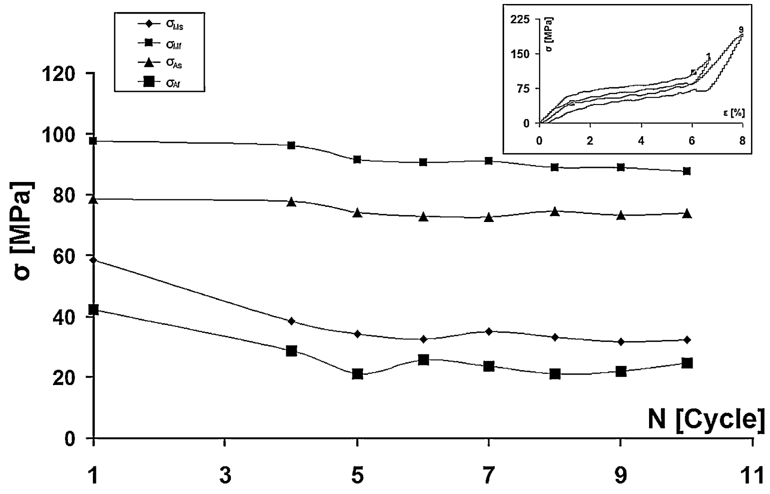

Fig. 5. Start and finish stresses as the function of the number of cycles, from the σ–ε curves (shown in the insert).

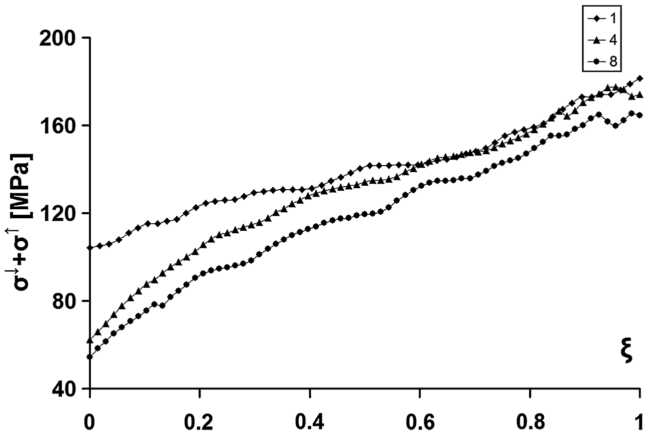

Fig. 6. $\sigma\downarrow(\xi)+\sigma\uparrow(\xi)$ versus ξ at different N cycles.

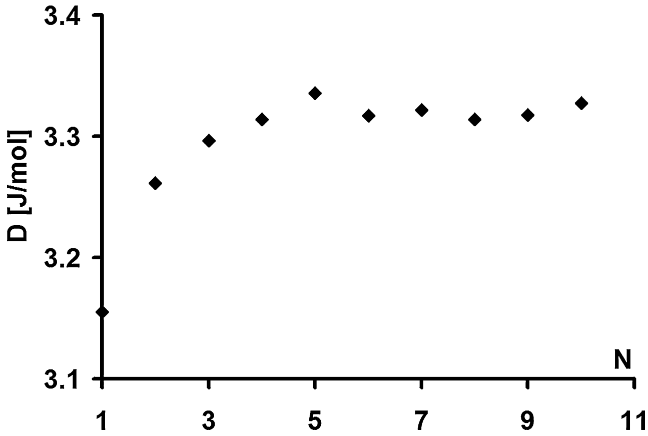

Fig. 8. Cycle number dependence of the total dissipative energy.

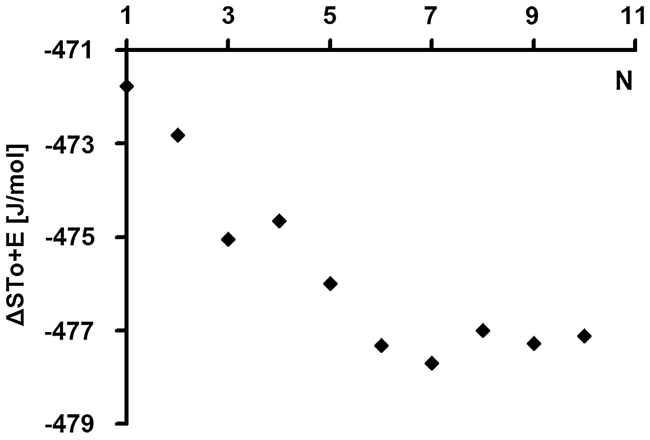

Fig. 7. Cycle number dependence of the total elastic energy.

3.2. Stress–strain measurements

For the determination of the N dependence of the total dissipative and elastic energies per one cycle one has to use the following relations (derived similarly as Eq. (1) for the thermal hysteresis loops [2]):

$$\sigma^{A/M}(\xi)=\sigma_o(T)-[d(\xi)+e(\xi)]/V\varepsilon^{\mathrm{tr}}(T)$$

$$\sigma^{M/A}(\xi)=\sigma_o(T)-[d(\xi)+e(\xi)]/V\varepsilon^{\mathrm{tr}}(T) \qquad (3)$$

where the another form of the Clausius–Clapeyron relation holds for the temperature dependence of the equilibrium transformation stress, σ_{o}, as

$$\sigma_o T=-(\delta s/V\varepsilon^{\mathrm{tr}}(T))[T-T_o(0)] \qquad (4)$$

Here the transformation strain, $\varepsilon^{\mathrm{tr}}$, depends on the temperature, and should be taken at that fixed T at which the ε–σ loop is taken (for the temperature dependence of $\varepsilon^{\mathrm{tr}}$ see Fig. 3b in [10]).

The inset in Fig. 5 shows the stress–strain curves for two cycles, at 373 K (starting from the austenite phase, $T > A_s$). There is some small increase in the transformation strain by increasing the number of cycles. In Fig. 5 the start and finish stresses are plotted versus the number of cycles and it can be seen that there is some decrease in σ_{Ms} and σ_{Af} by the increase of the cycle numbers before reaching a saturation. Fig. 6 shows the $\sigma^{\mathrm{A/M}}(\xi)+\sigma^{\mathrm{M/A}}(\xi)$ function, which is proportional to $2e(\xi)$ (see Eqs. (3) and (4)). Fig. 7 shows the N dependence of the total elastic energy, obtained by the integration of the curves shown in Fig. 6.

The total dissipative energy (calculated from the integrals of the $\sigma^{\mathrm{A/M}}(\xi)$–$\sigma^{\mathrm{M/A}}(\xi)$ functions) versus N is shown in Fig. 8. In the calculations of E and D the dependence of $\varepsilon^{\mathrm{tr}}$ on N was neglected and $\varepsilon^{\mathrm{tr}} = 0.046$ was taken (as red out from the insert in Fig. 5), which is also in a good accordance with the value obtained from the temperature dependence of $\varepsilon^{\mathrm{tr}}$ at 373 K (see Fig. 3b of [10]). It is clear that the elastic energy decreases while the dissipative energy increases by increasing the number of cycles.

4. Discussion

As it can be seen in Figs. 2, 3 and 5 both the thermal and mechanical cycling causes some changes in the hysteretic loops: after a fast shift in the first few cycles the stress–strain and strain-temperature responses stabilize.

In thermal cycling the elastic energy, *E*, as well as the dissipative energy, *D* per one cycle increases as well as decreases, respectively with increasing number of cycles, while in mechanical cycling there is an opposite tendency. These changes are inevitably related to the change in the martensite variant structure during cycling.

In thermal cycling, where self-accommodated martensite variant structure develops, with increasing numbers of *N*, due to some "learning process in nucleation of similar variants" at different places, the martensite variant structure stabilizes and interestingly in this process *E* increases (by about 2.5%) and *D* decreases (by about 50%).

In mechanical cycling it is expected that the learning process can lead to an increased number of nucleation of preferentially oriented (according to the direction of the applied uniaxial stress) martensite variants. This decreased *E* and increased *D* by about 1% and 6%, respectively.

It was pointed out in [11] that in general there are two energy dissipative processes: the first is related to the frictional interfacial motion, while the second is due to the dissipation of the stored elastic energy when the coherency strains at the martensite/austenite interface relax. Assuming the first contribution independent of *N*, the increase/decrease of *E* can be accompanied by a decrease/increase in *D*, but for a deeper understanding detailed microscopic investigations of the variant structure and the interfaces, similarly as e.g. was done in [11], are necessary.

In order to underline the importance of understanding of the detailed microscopic mechanisms it is worth mentioning that in general two types of interfacial properties dominate the behavior of martensites [12–14]; (i) phase front(s) between coexisting austenite and martensite regions and (ii) interfaces between different martensite variants. From this point of view in thermal cycles the motions of interfaces between the austenite and martensite should dominate, while the motion of interfaces between martensite variants can also considerably contribute the energetic processes. Furthermore, it has been shown that in martensitic transitions two types of criticality (connected to the jerky motion of the interfaces) can be observed depending on the driving mechanism [15–17]: either a classical criticality (requiring fine tuning of disorder: disorder induced criticality) or disorder independent, self-organized criticality [18,19]. Disorder induced criticality occurs in pure thermally induced martenstic transition; in this case dislocations are formed during the transformation process and the amount if this disorder can be controlled by cycling through the transition [20]. Indeed the effect of cycling on acoustic emission parameters was investigated in different Cu-based shape memory alloys and it was concluded [20] that, after enough cycling the exponent of the amplitude distribution was independent of composition, transition temperature, heat treatment and even whether or not the system was single or polycrystalline and depended only on the symmetry of the low temperature phase. On the other hand no significant cycling evolution has been found in acoustic emission experiments during *stress-driven* martensitic transformation to a single variant martensite structure in $CuZn_{15.7}Al_{16.1}$ single crystals [21] and it was concluded that no tendency to criticality occurs during the transformation to a single variant martensite (in contrast to transformation to a multi variant structure).

5. Conclusions

It is shown that during mechanical and thermal cycling of CuAl(11.5wt%)Ni(5.0wt%) single crystal shame memory alloy the elastic and dissipative energy contributions to the β/β' phase transformation have the following dependence on the number of cycles, *N*;

- Both the dissipative, *D*, and elastic energy, *E*, (per one cycle) show a definite dependence on the number of cycles in the first few cycles and then a saturation value is reached with increasing *N*. i.e. the stress–strain and strain-temperature responses stabilize.
- In thermal cycling the elastic energy, *E*, as well as the dissipative energy, *D* per one cycle increases as well as decreases, respectively with increasing number of cycles, while in mechanical cycling there is an opposite tendency. These changes are related to the change in the martensite variant structure during cycling. In thermal cycling *E* increased by about 12 J/mol, and *D* decreased by about 6 J/mol. On the other hand for mechanical cycling *E* decreased by about 6 J/mol and *D* increased by about 0.2 J/mol.

Acknowledgments

This work was supported by the Hungarian Scientific Research Fund (OTKA) Project No. K 84065 as well as by TAMOP-4.2.2/B-10/1-2010-0024 project from the European Social Fund.

References

[1] Z. Palánki, L. Daróczi, D.L. Beke, Mater. Trans. A 46 (2005) 978–982.
2 D.L. Beke, L. Daróczi, Z. Palánki, On relations between the transformation temperatures, stresses, pressures and magnetic fields in shape memory alloys, in: S. Miyazaki (Ed.), Proc. of Int. Conf. on Shape memory and Superleastic Technologies, 2007 Tsukuba, Japan, ASM International, Materials Park, Ohio, 2008, p. 607-614.
[3] T.W. Duerig, K.N. Melton, D. Stockel, C.M. Wayman (Eds.), Engineering Aspects of Shape Memory Alloys, Butterworth-Heinemann, London, 1990.
[4] A.R. Pelton, D. Hodgson, T.W. Duerig (Eds.), Shape Memory and Superelastic Technologies Proceeding of SMST-94, Asilomar, USA, 1994.
[5] K. Otsuka, C.M. Wayman (Eds.), Shape Memory Materials, Cambridge University Press, Cambridge, UK, 1998.
[6] J. Ortín, A. Planes, Acta Metallurgica 36 (8) (1988) 1873–1889.
[7] L. Delaey, Diffusionless transformation, in: R.W. Cahn, P. Haasen, E.J. Kramer (Eds.), Materials Science and Technology – A Comprehensive Treatment Vol. 5, in: P. Haasen (Ed.), Phase Transformations in Materials, Weinheim, VCH, 1991, p. 339 (Chapter 5).
[8] K. Otsuka, X. Ren, Prog. Mater. Sci. 50 (2005) 511.
[9] A. Planes, T. Castan, J. Ortin, L. Delay, J. Appl. Phys. 66 (6) (1989) 2342.
[10] T.Y. El Rasasi, L. Daróczi, D.L. Beke, Intermetallics 18 (6) (2010) 1137–1142.
[11] R.F. Hamilton, H. Sehitoglu, Y. Chumlyakov, H.J. Mayer, Acta Materialia 52 (11) (2004) 3383–3402.
[12] E.K.H. Salje, H. Zhang, A. Planes, X. Moya, J. Phys.: Condens. Matter. 20 (2008) 275216.
[13] E.K.H. Salje, H. Zhang, D. Schryvers, B. Bartova, Appl. Phys. Lett. 90 (2007) 221903.
[14] E.K.H. Salje, Solid State Phenom. 172–174 (2011) 3–12.
[15] E. Vives, D. Soto-Parra, L. Manosa, R. Romero, A. Planes, Phys. Rev. B 80 (2009) 180101(R).
[16] E. Vives, D. Soto-Parra, L. Manosa, R. Romero, A. Planes, Phys. Rev. B 84 (2011) 060101(R).
[17] F.J. Perez, L. Truskinovsky, G. Zanotto, Phys. Rev. Lett. 101 (2008) 230601.
[18] J. Van Humbeeck, J. Alloys Compd. 355 (2003) 58–64.
[19] D.Z. Liu, D. Dunne, Scr. Mater. 48 (2003) 1611–1615.
[20] M.C. Gallardo, J. Manchado, F.J. Romero, J. del Cerro, E.K.H. Salje, A. Planes, E. Vives, Phys. Rev. B 81 (2010) 174102.
[21] E. Bonnot, E. Vives, L. Manosa, A. Planes, R. Romero, Phys. Rev. B 78 (2008) 094104.